Determination of surface-wave phase velocities across USArray from noise and Aki's spectral formulation

Göran Ekström,[1] Geoffrey A. Abers,[1] and Spahr C. Webb[1]

Received 11 May 2009; revised 27 July 2009; accepted 6 August 2009; published 16 September 2009.

[1] We use expressions for the cross-correlation of stochastic surface waves originally derived by Aki (1957) to develop an algorithm for determining inter-station phase-velocity measurements from continuous seismic data. In the frequency domain, the cross correlation of azimuthally isotropic noise is described by a Bessel function, and we associate zeros in the observed spectrum with zeros of the Bessel function to obtain phase-velocity estimates at discrete frequencies. Phase velocities derived in this way at several frequencies are joined to form a dispersion curve, which is then sampled to obtain phase-velocity estimates at arbitrary frequencies. We collect a set of dispersion curves for more than 30,000 station pairs of the transportable component of USArray, and derive Rayleigh wave phase-velocity maps at periods of 12 and 24 s for the western United States. The spectral method lends itself well to automation, and avoids limitations at short inter-station distances associated with time-domain methods.
Citation: Ekström, G., G. A. Abers, and S. C. Webb (2009), Determination of surface-wave phase velocities across USArray from noise and Aki's spectral formulation, *Geophys. Res. Lett.*, *36*, L18301, doi:10.1029/2009GL039131.

1. Introduction

[2] The cross correlation of continuous recordings of background ground motion for pairs of stations has recently been shown to be a powerful method for determining inter-station surface-wave group and phase velocities [*Shapiro and Campillo*, 2004; *Sabra et al.*, 2005; *Shapiro et al.*, 2005; *Yao et al.*, 2006; *Bensen et al.*, 2007; *Lin et al.*, 2008]. The method builds on correlation properties of random-noise signals that were first explored in seismology by *Aki* [1957] in a now-classic study of microseisms. With the growing availability of high-quality, continuous seismograms from regional seismic networks and temporary arrays, the systematic analysis of cross-correlation signals between stations within an array has led to the emergence of a powerful imaging technique dubbed Ambient Noise Tomography (ANT) [*Bensen et al.*, 2007]. The new techniques have allowed for regional mapping of Love and Rayleigh wave speeds at shorter periods than has previously been feasible with traditional earthquake-based methods, mainly because of the limited distribution of suitable earthquake sources. A striking example of the success of this technique is the set of phase- and group-velocity maps determined for the western United States from USArray Transportable Array (TA) data [*Lin et al.*, 2008], which provides high-resolution constraints on the elastic structure of the crust and uppermost mantle.

[3] Most recent approaches to the measurement of phase and group velocity from noise cross correlation have relied on the evolving understanding that the time-domain cross-correlation signal is closely related to the elastic Green function for a source located at one station and a receiver at the second. Based on this association, the Green function signal has been extracted from the cross correlation and subjected to standard group- and phase-velocity measurement techniques, such as Frequency-Time Analysis (FTAN) [*Dziewonski et al.*, 1969; *Levshin et al.*, 1989]. While these applications have been successful in obtaining dispersion information from the cross correlations, aspects of the analysis remain under discussion. In particular, the conditions under which the full Green function will emerge from the noise have been the subject of several studies [*Lobkis and Weaver*, 2001; *Snieder*, 2004; *Sánchez-Sesma and Campillo*, 2006]. In this paper, we return to *Aki*'s [1957] original formulation for the spectral correlation properties of noise, and develop a simple technique to extract phase-velocity measurements directly from the zero crossings of the real part of the correlation spectrum.

[4] With its focus on the correlation spectrum, our approach has features in common with the spatial autocorrelation (SPAC) method [e.g., *Cho et al.*, 2004; *Asten*, 2006], a technique developed to obtain local estimates of phase velocities and elastic structure from microtremors. The spectral formulation allows measurements to be collected for stations separated by distances of one wavelength or less. Distances shorter than two or three wavelengths have typically been avoided in time-domain studies, which depend on the far-field approximation in the interpretation of the Green function [*Shapiro et al.*, 2005; *Yao et al.*, 2006; *Yang et al.*, 2007; *Lin et al.*, 2008]. The new method lends itself to automation, and we have collected a large data set of dispersion curves for seismograms recorded on more than 600 stations of the USArray transportable array during 2006–2008. We validate the spectral approach and illustrate its potential by inverting Rayleigh wave phase-velocity measurements at periods of 12 s and 24 s to obtain phase-velocity maps of the western US, which we compare with the results of earlier studies.

2. Aki's Spectral Formulation

[5] *Aki* [1957] considered the correlation of stochastic horizontally propagating waves recorded at two stations and derived expressions for the azimuthally averaged

[1]Lamont-Doherty Earth Observatory, Earth Institute at Columbia University, Palisades, New York, USA.

0094-8276/09/2009GL039131

spectra for dispersive and polarized waves. A key result is equation (42) of *Aki* [1957],

$$\overline{\rho}(r,\omega_0) = J_0\left(\frac{\omega_0}{c(\omega_0)}r\right), \quad (1)$$

which states that the azimuthally averaged normalized cross spectrum $\overline{\rho}(r, \omega_0)$ for a receiver separation r and frequency ω_0 varies as J_0, the Bessel function of the first kind, where $c(\omega_0)$ is the phase velocity at frequency ω_0. Aki comments, "This formula clearly indicates that if one measures $\overline{\rho}(r, \omega_0)$ for a certain r and for various ω_0's, he can obtain the function $c(\omega_0)$, i.e., the dispersion curve of the wave for the corresponding range of frequency ω_0".

[6] *Cox* [1973] provided a derivation of the full form of the cross spectrum for a noise distribution with arbitrary azimuthal power density; the first term, corresponding to an isotropic noise field, is equivalent to that derived by *Aki* [1957]. In Part 3 of his 1957 paper, Aki argues, on the basis of similarities in the observed correlation functions derived from station pairs oriented at different azimuths, that the azimuthally averaged cross spectrum $\overline{\rho}(r, \omega_0)$ can be replaced in the analysis by the spectrum obtained for a single station pair. *Aki*'s [1957] observation underlies the assumption, now widely adopted, that the stochastic noise wavefield is sufficiently isotropic to make the leading term in the real part of the spectrum dominant.

3. Data and Methods

[7] In our algorithm, analysis and processing of the data for determination of individual phase-velocity measurements is accomplished in five steps: (1) time-frequency normalization of individual nine-hour-long seismograms, (2) calculation of station-pair cross spectra, (3) stacking of cross spectra for the period of observation, (4) identification of zero crossings in the real part of the spectrum, and (5) interpretation of zero crossings in terms of phase velocity.

[8] The original seismic signal is highly variable in time and the spectral amplitude varies by orders of magnitude across the broad-band period range of interest (~5–100 s). These variations reduce the validity of the assumption of a dominantly isotropic wavefield, leading to the need for some type of normalization. Other authors have accomplished this step by one-bit normalization [e.g., *Shapiro et al.*, 2005] and spectral whitening [*Bensen et al.*, 2007; *Harmon et al.*, 2008]. Here, we use a different approach, in which the original nine-hour-long seismogram is processed using a comb of 1-mHz-wide overlapping filters. The resulting nearly monochromatic signals are divided by their analytic time-domain envelopes to yield output signals of unit amplitude. These signals are then summed back together to form what we refer to as a time-frequency-normalized (TFN) seismogram.

[9] The TFN seismograms are tapered and transformed to the frequency domain, and the cross correlation of signals recorded at two stations is performed by spectral multiplication. Stacks are then formed by summing the available spectra, excluding those seismograms that overlap with significant earthquakes, here defined as any earthquake in the Global centroid-moment-tensor catalog [*Ekström et al.*, 2005]. Approximately one third of the records are eliminated by applying the absence-of-earthquake criterion.

[10] Figure 1 shows the stacked spectra for the TA station pairs D07A–B04A and D07A–C09A, located in Washington State and separated by 282 km and 145 km, respectively. The real parts of the spectra (dark blue) resemble a Bessel function in their oscillatory character, but the amplitudes of the peaks do not decrease monotonically with frequency as for J_0. This amplitude behavior is not surprising given the well-known peaks in the Earth's noise spectrum and the non-linear filtering involved in the time-frequency normalization. The imaginary component of the D07A–B04A spectrum is similar in amplitude to that of the real component, and also displays an oscillatory character. As described in detail by *Cox* [1973], the non-vanishing imaginary part of the cross spectrum is a consequence of the azimuthally non-uniform power of the noise.

[11] Because the amplitude of the real part of the spectrum depends on both the background noise spectrum and non-linear effects of the data processing, dispersion information cannot readily be deciphered from the detailed shape of the spectrum. The locations of the zero crossings in the spectrum should, however, be insensitive to variations in the spectral power of the background noise, and we choose to use the locations of these zero crossings as the dispersion observables. If ω_n denotes the frequency of the nth observed zero crossing and z_n denotes the nth zero of J_0, we can determine the corresponding phase velocity as

$$c(\omega_n) = \frac{\omega_n r}{z_n}, \quad (2)$$

following *Aki*'s [1957] approach. In observed spectra, association of a given zero with a particular zero crossing of J_0 may be difficult because noise in the spectrum can cause missed or extra zero crossings. To allow for this, we develop a set of phase-velocity estimates $c_m(\omega_n)$ based on equation (2), where

$$c_m(\omega_n) = \frac{\omega_n r}{z_{n+2m}}, \quad (3)$$

and m takes the values 0, ±1, ±2, . . ., indicating the number of missed or extra zero crossings.

[12] Figure 1 displays the locations of the zero crossings of the real spectra as points on a frequency *vs*. phase-velocity dispersion diagram. Connecting the positive-to-negative zero crossings and the negative-to-positive zero crossings generates two dispersion curves that can be assessed for consistency. Additional, trial dispersion curves are derived from the phase-velocity measurements resulting from different possible choices of m for each zero. At long periods, 'good' and 'bad' phase-velocity measurements can easily be identified by whether they fall within a realistic range (Figure 1). At shorter periods, the best criteria for evaluating the validity of phase-velocity estimates are the smoothness and continuity of the dispersion curves. By connecting zero crossings of the same kind (up or down), and allowing for extra or missed zero crossings at arbitrary locations in the spectrum, our algorithm generates a large suite of dispersion curves. It then discards all curves that have unacceptable phase-velocity values or step-like veloc-

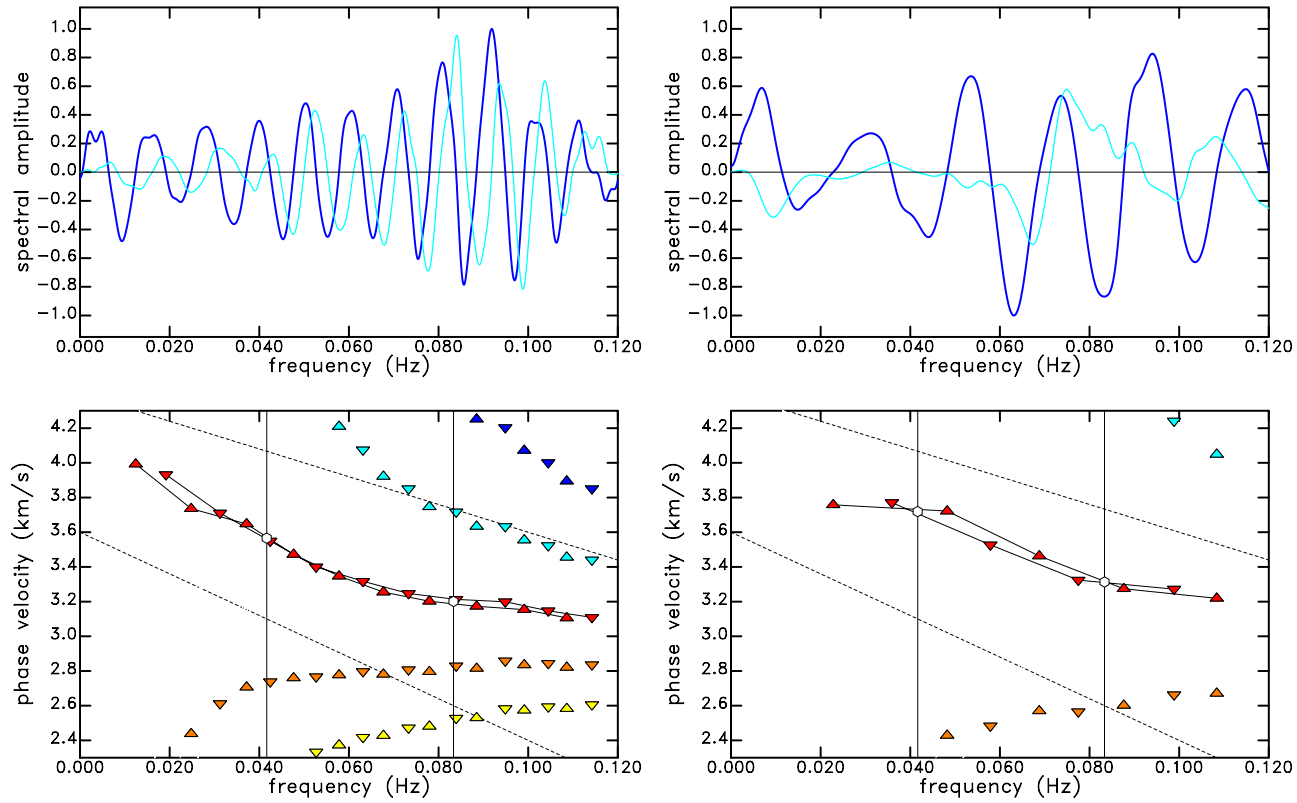

Figure 1. (top) Stacked spectra for the station pairs (left) D07A–B04A and (right) D07A–C09A. Dark blue lines show the real parts of the spectra and light blue lines show the imaginary parts. The stations are separated by 282 km (Figure 1, top left) and 145 km (Figure 1, top right), and the stacks were formed from 6988 h (Figure 1, top left) and 8324 h (Figure 1, top right) of earthquake-free cross-correlated seismograms. The spectra are tapered to 0 below 0.005 Hz. (bottom) Dispersion diagrams showing the phase-velocity values derived from the zero crossings of the spectra above. Downward triangles show zero crossings from positive to negative, upward triangles show crossings from negative to positive. Red triangles correspond to $m = 0$, with no missing or extra zeros. Orange triangles correspond to $m = 1$; yellow to $m = 2$; light blue to $m = -1$; and dark blue to $m = -2$. Dashed lines outline the region used to define acceptable phase velocities at each frequency. Black lines connect upward- and downward-pointing triangles to define the dispersion curves that are sampled at discrete frequencies for the subsequent analysis. Thin vertical lines and hexagons show the frequencies and phase velocities corresponding to the samples at 12 s and 24 s.

ity changes between adjacent zero crossings. The remaining dispersion curves (one connecting up-crossing zeros and one connecting down-crossing zeros) are then evaluated at the desired period. The difference between the phase velocities of the two curves at each sampled frequency is saved and used as a quality criterion.

4. Application to USArray Data

[13] We applied the method described in section 3 to vertical-component seismograms recorded by the USArray TA during 2006–2008. Continuous data from all available stations were collected, and cross spectra were calculated and stacked for all station pairs with separations smaller than 300 km. The automated algorithm was used to determine dispersion curves from the zeros of the spectra.

[14] To assess the quality of the dispersion curves and validate the spectral approach, we collected phase-velocity measurements at 12-s period and used them in an inversion for a phase-velocity map for the area covered by the TA through the end of 2008. We selected paths in the distance range 50–300 km, and used only those stacked spectra that included 2000 or more hours of data. Measurements for which the two (up and down) dispersion curves differed by more than 0.25 km s^{-1} at 12 s were not included in the inversion. The phase-velocity map was parameterized using 0.25×0.25-degree pixels. A small amount of damping was applied in the inversion to minimize model roughness. Figure 2 shows the result. Retrieved phase-velocity variations range from −16% to +10% with respect to the average velocity of 3.21 km s^{-1}. The retrieved map reduces the data variance by 65% with respect to the best-fitting uniform phase-velocity model, reflecting the high level of internal consistency between the measurements. Prominent large-amplitude features in the model include very slow velocities associated with the Great Valley in California, the Olympic Peninsula in Washington, and Yellowstone, and fast anomalies associated with the Sierra Nevada in California. The northern sections of the imaged area and portions of the Colorado Plateau also show strong fast velocities. The similarities between this map and that of *Lin et al.* [2008] are striking. The spatial correlation of the two maps is 0.85,

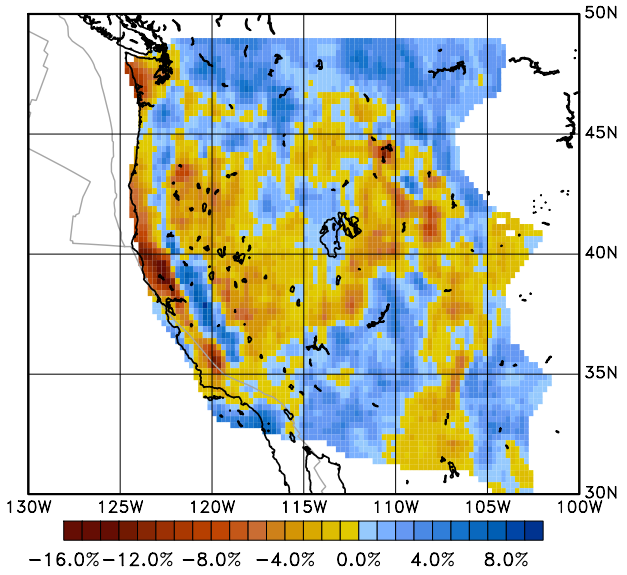

Figure 2. Phase-velocity map of 12-second Rayleigh waves for the western United States. The map is parameterized using 0.25 × 0.25-degree pixels. The total number of data is 27,528 and the variance reduction with respect to the best-fitting uniform velocity is 65%. Only pixels with at least one crossing ray are colored. Velocity variations are plotted with respect to the mean velocity of 3.21 km s^{-1}.

and the mean phase velocities differ by less than 0.01 km s^{-1}. This similarity suggests that the spectral approach can profitably be applied to the surface-wave tomography problem.

5. Discussion

[15] One of the potential benefits of the spectral method is that there is no theoretical limit on its applicability at small station separations. In contrast, time-domain methods commonly restrict the analysis to path lengths greater than two wavelengths [*Shapiro et al.*, 2005] or three wavelengths (λ) [*Bensen et al.*, 2007; *Harmon et al.*, 2008; *Lin et al.*, 2008; *Yang et al.*, 2007; *Yao et al.*, 2006], since a far-field approximation is used in the interpretation of the time-domain signal. In principle, the first zero crossing of the cross spectrum, which occurs at a station separation corresponding to 0.38 λ, could be used to obtain a phase-velocity measurement. In this study, we have not explored sub-wavelength possibilities, but we have investigated the robustness of results derived from short-separation dispersion measurements.

[16] We divided our measurements of phase velocity at 24-s period into distinct data sets corresponding to two distance ranges, 100 km $\leq r \leq$ 200 km ($1.2\lambda \leq r \leq 2.35\lambda$), and 200 km $\leq r \leq$ 300 km ($2.35\lambda \leq r \leq 3.5\lambda$). We inverted the two data sets separately for phase velocity maps. Figure 3 shows the results. The two data sets yield very similar maps, with average velocities of 3.56 km s^{-1} and anomaly patterns that agree well in location and strength. Both maps reduce the variance of the data by more than 80% with respect to the best-fitting uniform velocity. The spatial correlations with the 24-s phase-velocity map of *Lin et al.* [2008] are 0.87 and 0.90, and the mean phase velocities of the three maps differ by less than 0.01 km s^{-1}. These results demonstrate that the spectral measurements are robust and consistent even for very short station separations.

6. Conclusions

[17] We have developed an algorithm to extract dispersion data from continuous seismic records, using *Aki*'s [1957] original expression for the cross correlation of stochastic surface waves. We focus on the zero crossings of the real cross-correlation spectrum because they are likely to be insensitive to the power spectrum of the background noise and the non-linear filtering of the original signal, and because their identification leads to a simple means for constructing dispersion curves. The determination of separate dispersion curves for the two families of zeros (up and down) allows us to develop a simple criterion for the quality of an individual phase-velocity measurement, and to automate the entire analysis.

[18] Inversion of measurements at 12-s period results in phase-velocity maps of the western US that reflect heterogeneity of crustal structure at lengthscales of ∼100 km and compare well to earlier results. Inversions of measurements at 24 s indicate that the method produces robust and unbiased measurements at distances smaller than 2λ, suggesting that the spectral method may be useful for extending the noise-correlation approach to shorter inter-station distances at a given period.

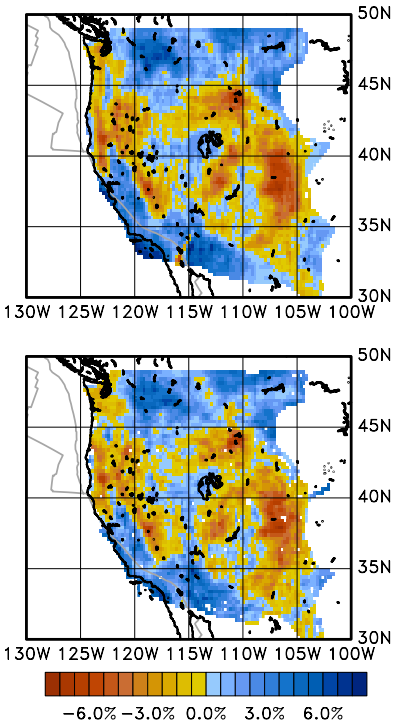

Figure 3. Phase-velocity maps of 24-second Rayleigh waves for the western United States. (top) Inversion result based on paths with lengths 200 km $\leq r \leq$ 300 km (5,322 measurements). (bottom) Inversion results based on paths with lengths 100 km $\leq r \leq$ 200 km (4,644 measurements). For both maps, the variance reduction is greater than 80% and the mean velocity is 3.56 km s^{-1}.

[19] There is no reason to expect the spectral method to be less sensitive to deviations from the assumed isotropy of the stochastic wavefield than common time-domain approaches, since the real part of the spectrum is equivalent to the even part of the time-domain cross correlation. With an improved characterization of the azimuthal variation of the noise, the spectral approach could be refined using expressions similar to those of *Cox* [1973], which would also allow the use of the imaginary part of the spectrum.

[20] The consistency of the maps derived here with those of earlier studies, as well as the high reduction of variance obtained in the inversions, suggests that the stochastic wavefield, at the periods considered, is indeed sufficiently isotropic to allow proper phase velocities to be determined. In modern studies exploiting data from homogeneous arrays such as USArray, the averaging originally assumed by *Aki* [1957, equation (42)] may in practice occur in the azimuthal averaging of many paths in the tomographic inversion.

[21] **Acknowledgments.** The seismograms used for this research were retrieved from the IRIS Data Management Center (DMC) and come primarily from the Transportable Array of USArray, the Berkeley Digital Seismic Network, and the Caltech Digital Seismic Network. We are grateful to the operators of these networks for the high-quality data that made this study possible, and to the IRIS DMC for making them easily available. We thank Fan-Chi Lin for providing his phase-velocity maps, and Jeroen Ritsema, Meredith Nettles, Josh Calkins, and an anonymous reviewer for comments that helped improve the manuscript.

References

Aki, K. (1957), Space and time spectra of stationary waves with special reference to microtremors, *Bull. Earthquake Res. Inst. Univ. Tokyo*, *35*, 415–456.

Asten, M. W. (2006), On bias and noise in passive seismic data from finite circular array data processed using SPAC methods, *Geophysics*, *71*, V153–V162, doi:10.1190/1.2345054.

Bensen, G. D., M. H. Ritzwoller, M. P. Barmin, A. L. Levshin, F. Lin, M. P. Moschetti, N. M. Shapiro, and Y. Yang (2007), Processing seismic ambient noise data to obtain reliable broad-band surface wave dispersion measurements, *Geophys. J. Int.*, *169*, 1239–1260, doi:10.1111/j.1365-1246X.2007.03374.x.

Cho, I., T. Tada, and Y. Shinozaki (2004), A new method to determine phase velocities of Rayleigh waves from microseisms, *Geophysics*, *69*, 1535–1561.

Cox, H. (1973), Spatial correlation in arbitrary noise fields with applications to ambient sea noise, *J. Acoust. Soc. Am.*, *54*, 1289–1301.

Dziewonski, A. M., S. Bloch, and M. Landisman (1969), A technique for the analysis of transient seismic signals, *Bull. Seismol. Soc. Am.*, *59*, 427–444.

Ekström, G., A. M. Dziewonski, N. N. Maternovskaya, and M. Nettles (2005), Global seismicity of 2003: Centroid-moment tensor solutions for 1087 earthquakes, *Phys. Earth Planet. Inter.*, *148*, 327–351.

Harmon, N., P. Gerstoft, C. A. Rychert, G. A. Abers, M. Salas de la Cruz, and K. M. Fischer (2008), Phase velocities from seismic noise using beamforming and cross correlation in Costa Rica and Nicaragua, *Geophys. Res. Lett.*, *35*, L19303, doi:10.1029/2008GL035387.

Levshin, A. L., T. L. Yanovskaya, A. V. Lander, B. G. Bukchin, M. P. Barmin, L. I. Ratnikova, and E. N. Its (1989), *Seismic Surface Waves in a Laterally Inhomogeneous Earth*, edited by V. I. Keilis-Borok, Kluwer Acad., Norwell, Mass.

Lin, F., M. P. Moschetti, and M. H. Ritzwoller (2008), Surface wave tomography of the western United States from ambient seismic noise: Rayleigh and Love wave phase velocity maps, *Geophys. J. Int.*, *173*, 281–298, doi:10.1111/j1365-1246X.2008.3720.x.

Lobkis, O. I., and R. L. Weaver (2001), On the emergence of the Green's function in the correlations of a diffuse field, *J. Acoust. Soc. Am.*, *110*, 3011–3017.

Sabra, K. G., P. Gerstoft, P. Roux, W. A. Kuperman, and M. C. Fehler (2005), Surface wave tomography from microseisms in southern California, *Geophys. Res. Lett.*, *32*, L14311, doi:10.1029/2005GL023155.

Sánchez-Sesma, F. J., and M. Campillo (2006), Retrieval of the Green's function from cross correlation: The canonical elastic problem, *Bull. Seismol. Soc. Am.*, *96*, 1182–1191.

Shapiro, N. M., and M. Campillo (2004), Emergence of broadband Rayleigh waves from correlations of the ambient seismic noise, *Geophys. Res. Lett.*, *31*, L07614, doi:10.1029/2004GL019491.

Shapiro, N. M., M. Campillo, L. Stehly, and M. Ritzwoller (2005), High resolution surface wave tomography from ambient seismic noise, *Science*, *307*, 1615–1618.

Snieder, R. (2004), Extracting the Green's function from the correlation of coda waves: A derivation based on stationary phase, *Phys. Rev. E*, *69*, 046610, doi:10.1103/PhysRevE.1169.046610.

Yang, Y., M. H. Ritzwoller, A. L. Levshin, and N. M. Shapiro (2007), Ambient noise Rayleigh wave tomography across Europe, *Geophys. J. Int.*, *168*, 259–274, doi:10.1111/j.1365-246X.2006.03203.x.

Yao, H., R. D. van der Hilst, and M. V. de Hoop (2006), Surface-wave array tomography in SE Tibet from ambient seismic noise and two-station analysis—I. Phase velocity maps, *Geophys. J. Int.*, *166*, 732–744, doi:710.1111/j.1365-1246X.2006.03028.x.

G. A. Abers, G. Ekström, and S. C. Webb, Lamont-Doherty Earth Observatory, Earth Institute at Columbia University, 61 Route 9W, Palisades, NY 10964, USA. (ekstrom@ldeo.columbia.edu)